



Lasers in Manufacturing Conference 2021

## Excimer laser sintering of ceramic thin films for solid state batteries

Matthias Trenn<sup>a,\*</sup>, Linda C. Hoff<sup>a</sup>, Ralph Delmdahl<sup>b</sup>,  
Matthias Greiber<sup>a</sup>, Karsten Lange<sup>a</sup>, Christian Vedder<sup>a</sup>

<sup>a</sup>Fraunhofer Institute for Laser Technology (ILT), Steinbachstraße 15, 52074 Aachen, Germany

<sup>b</sup>Coherent LaserSystems GmbH & Co. KG, Göttingen, Hans-Böckler-Straße 12, 37079 Göttingen, Germany

---

### Abstract

The geopolitical dependence on limited fossil resources and the increasing number of environmental disasters are enormous challenges for today's society. An important element to overcome these essential problems is to increase the performance of energy storage systems and the efficiency of energy conversion devices. A promising solution are ceramic solid-state batteries providing a high level of safety and energy density. One of the challenges on the way to high volume production is the demand of a temperature-sensitive thin-film sintering process step, where the conventional sintering process is limited. The production of solid-state batteries demanding high standards on new production technologies. In this paper, a new highly scalable excimer laser-based sintering process of ceramic thin films is presented. The nanosecond pulses selectively melt the material at the surface of the powder grains. Due to the short 248 nm laser wavelength, sintering depths of only 4 - 8  $\mu\text{m}$  can be achieved. In the process, the crystalline phase of the powder and thus also the electrochemical properties of the layer are retained.

Keywords: excimer laser; thin film sintering; ceramic sintering; solid-state batteries; large-area processing

---

\* Corresponding author. Tel.: +49 2418906-449; fax: +49241/8906-121  
E-mail address: matthias.trenn@ilt.fraunhofer.de

## 1. Introduction

Climate change and energy transition to renewable energies is one of the central challenges of today's politics, society, and science. The need to store energy from renewable sources and the ongoing electrification of mobility increase the demand for safe batteries with high energy density. Currently, lithium-ion batteries are widely used and show promising application possibilities. However, the lack of safety, the limited energy storage capacity and the suffer from raw materials availability demand for new, safe, and more efficient alternatives. Ceramic solid-state batteries (CSSB) are promising candidates for future applications. They are inherently safe due to the lack of flammable organic components and offer the potential to significantly improve the energy density through the lithium metal anode [1]. Instead of a porous separator soaked with liquid electrolyte, CSSBs use a solid ceramic electrolyte, which is on the one hand electrical insulating and on the other hand ion conductive (Fig. 1).

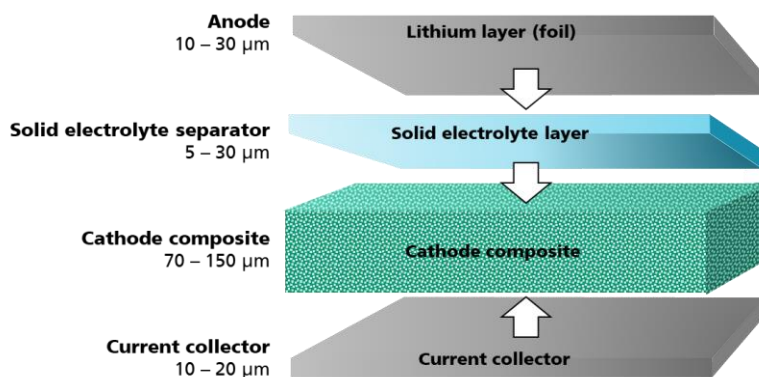


Fig. 1. Structure and components of a ceramic solid-state battery consisting of a thick cathode layer, a thin-film electrolyte and a Lithium metal anode. Based on [1].

Even though the advantages of CSSBs have been theoretically proven and first prototypes have already been produced, upscaling from laboratory research scale to industrial mass production raises multiple challenges and requirements. This applies especially for the electrolyte layer. One promising material, which meets the electrochemical requirements, is Lithium Lanthanum Zirconate (LLZ). With a total ion conductivity of  $\sigma_{\text{ION}} > 10^{-4}$  S/cm at room temperature and its wide electrochemical stability window, CSSBs based on LLZ could provide higher energy densities than common Lithium ion batteries by using high voltage cathodes and metallic Lithium anodes. The resulting lifetime would be longer due to a minimization of the electrolyte-related degradation during cycling [2]. Furthermore, the resistance of the ion conducting electrolyte can be additionally decreased by reducing the layer thickness of the LLZ. Therefore, a depth-resolved and temperature-controlled sintering process is required to avoid on the one hand thermal damage of the underlying cathode and on the other hand maintain the Li-ion conductive crystalline structure of the LLZ layer.

In this paper, a new highly scalable excimer laser-based sintering process of LLZ thin film is presented. For the required depth resolved sintering, Krypton Fluoride excimer laser radiation was used. With a wavelength of 248 nm, the optical penetration depth and thus the sintering depth of a ceramic powder coating is only a few microns. Additionally, the nanoseconds pulses lead to a rapid surface selective melting/sintering process, where thermal diffusion is avoided due to the short interaction time between laser pulse and material. Thus,

the underlying layer is prevented of thermal damage. The challenge of the presented sintering process is to ensure the phase stability of the LLZ. To achieve this, the laser parameters in terms of the fluence and the number of pulses were adjusted.

Also, the used excimer laser and optical system from Coherent bridges the gap between research lab-scale manufacturing and industrial mass production. With a scalable line beam profile of up to over one meter width, large area processing is already possible today.

## 2. Experimental Setup

### 2.1. Material

For the investigated ceramic electrolyte material,  $\text{Li}_7\text{La}_3\text{Zr}_2\text{O}_{12}$  (LLZ) doped with Tantalum (Ta) was used. The particle sizes of the powder are  $D_{10} = 0.05 \mu\text{m}$ ,  $D_{50} = 0.15 \mu\text{m}$ ,  $D_{90} = 0.4 \mu\text{m}$ . To enhance the laser sintering process,  $\text{Li}_3\text{BO}_3$  (LBO) was added to the powder mixture as a sinter additive with a melting point around  $700^\circ\text{C}$  [3]. Layers of about  $100 \mu\text{m}$  powder thickness on a steel substrate were produced by screen-printing. The particles were processed as a coating with terpineol as solvent and ethyl cellulose as binder, resulting in a paste with a powder loading of 30 wt%. In the final process step before sintering, the samples were dried for 3 h at  $40^\circ\text{C}$  in an oven to remove the solvent and subsequently heated up from  $20^\circ\text{C}$  to  $550^\circ\text{C}$  with a heating rate of 2 K/min for binder removal.

### 2.2. Laser source and optical system

The used laser beam source was the Coherent LEAP excimer laser. Since excimer lasers are the only native laser light sources in the UV spectrum, they are the only practical source of high-power UV laser technology. Hence, UV excimer lasers are predestined for modifying micro- and nanometer-scale layers in large-scale processes. The excimer laser delivers stabilized output power of 150 W even for a large number of pulses at 1 Joule pulse energy (typ. 0.5 %, sigma) and 150 Hz maximum repetition rate, respectively (Fig. 2).

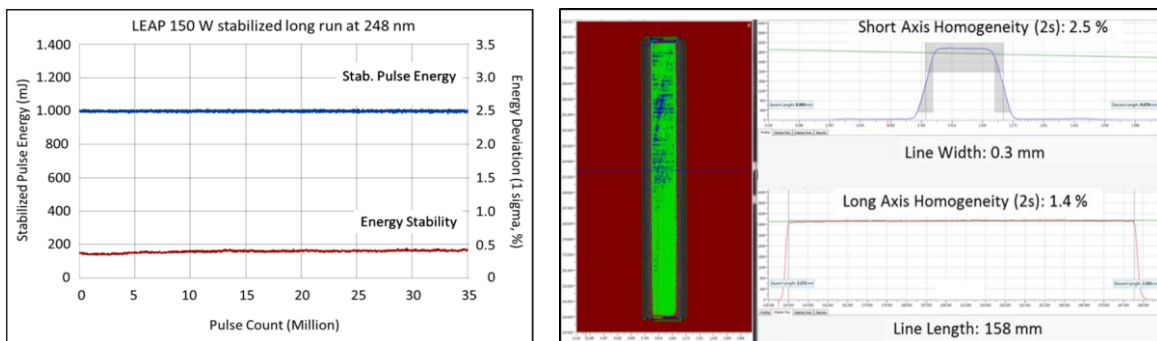


Fig. 2. Left: the long-term pulse energy stability of 35 million pulses at 1 J (blue line) and the energy deviation (red line) are depicted. Right: a false color CCD camera image of the line beam 155 and the respective top-hat profile cross sections obtained along the short beam axis and the long beam axis are shown.

This long-term stabilized excimer laser is now combined with Coherent's LineBeam155 optical system ensuring high reproducibility and quality when processing thin films on larger substrates. The beam projection design of the 248 nm line beam system provides a unique  $1.2 \text{ J/cm}^2$  fluence in the substrate plane and a nominal beam size of  $155 \text{ mm} \times 0.4 \text{ mm}$ . In Figure 2, a two-dimensional CCD camera image of the line beam

recorded in the substrate plane is shown together with the cross sections obtained along the short beam axis and the long beam axis. It can be clearly seen from the cross sections that both the short and the long beam axis are shaped into a flat-top profile. Two sigma homogeneity values of 2.5 % for the short axis and 1.4 % of the long axis are easily achieved with the LEAP line beam system. The slight flat-top tilt which is visible in the short axis cross section can be deliberately adjusted from positive to negative angles to optimize laser material interaction during ablative scanning applications. On the basis of 1 J/pulse excimer laser output as provided by the LEAP and taking into account the overall optical efficiency of the line beam system of nearly 70%, a line length of 158 mm (FWHM) (nominal value of 155 mm) and a line width of 0.4 mm (FWHM) with a homogeneous maximum fluence of 1.2 J/pulse is achievable. [4]

### 2.3. Analysis technology

For the analyses of the sintering process and the sintered LLZ material, three aspects are of particular interest:

1. The sintering degree determining the link between the particles.
2. The sintering depth, which is specified by analyzing the cross-section.
3. The crystal structure of the treated material, which is an indication for the Li-ion conductivity.

In this work, the sintering degree and the sintering depth is investigated with the scanning electron microscope (SEM) Leo 1455 EP by Carl Zeiss AG. The crystal structure was measured by X-ray diffraction with a Bruker Advance D8 X-ray diffractometer having a Cu X-ray tube ( $\lambda = 1.45059 \text{ \AA}$ ). As measurement procedure a Bragg-Brentano geometry between the angles of  $15^\circ$  and  $60^\circ$  was used.

### 3. Results

In Figure 3, the SEM images of the laser-sintered surfaces of the LLZ layers with increasing energy input are presented. From the sample a) to the c), the fluence was increased from  $230.4 \text{ mJ/cm}^2$  up to  $1239.0 \text{ mJ/cm}^2$ . From d) – f), the number of pulses was raised from 250 per mm up to 2000 pulses per mm scanning path at constant repetition rate of 100 Hz.

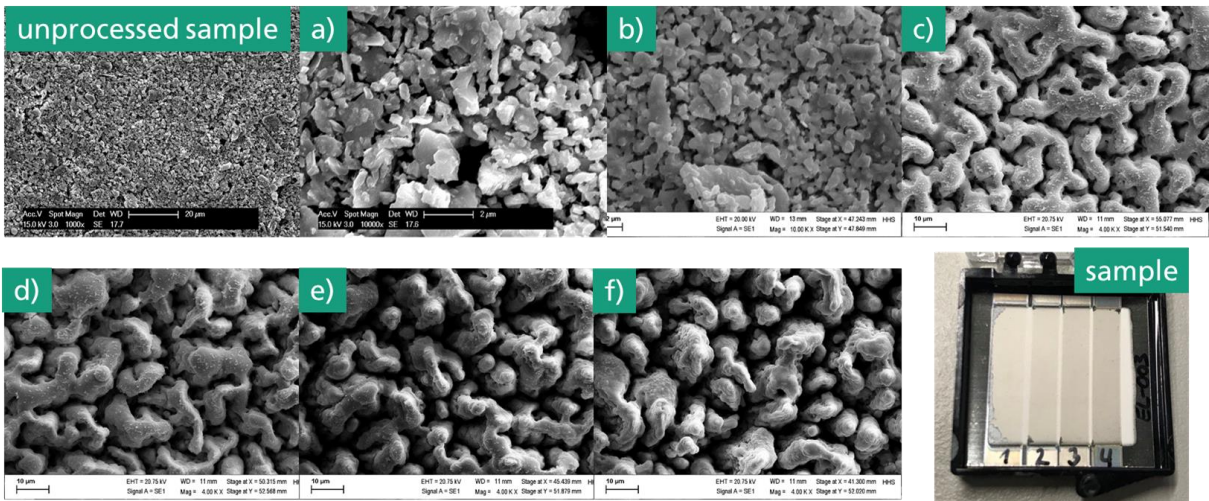


Fig. 3. SEM images of the sintered LLZ surfaces. First, the fluence was increased at constant processing parameters (a,  $230.4 \text{ mJ/cm}^2$ ; b,  $288 \text{ mJ/cm}^2$ ; c,  $1239 \text{ mJ/cm}^2$ ). From d) - f), the number of pulses was raised at constant repetition rate of 100 Hz.

The particles even for small fluences show sintering behavior. This means, the particle shells are melted but the particle form is nearly preserved (a and b). With increasing energy input, more of the particles are sintered, form bigger particles until a coral-like structured is generated. This formation results on the one hand from a melting process, which is becoming more dominate with higher fluences, and on the other hand from an anisotropic shrinking of the powder layer. At a high number of pulses (e and f), melting dynamics can be recognized forming dots/pikes on the surface.

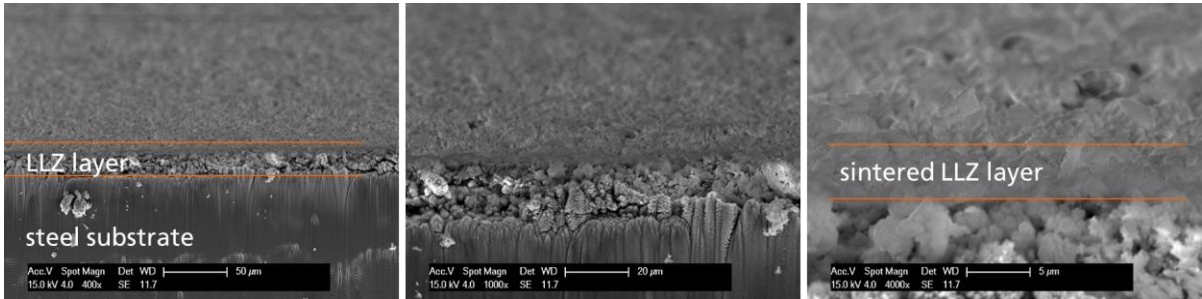


Fig. 4. SEM images of the cross section of sintered LLZ powder material on steel substrate. The sintered layer is labeled.

In Figure 4, the cross section of the laser sintered sample c) is presented. The cross section can be divided into three parts: the steel substrate at the bottom, the particular LLZ layer and a laser sintered LLZ layer on top. In the image on the right hand side, the sintered layer thickness of 4 – 8  $\mu\text{m}$  is recognisable. The anisotropic layer thickness is a result of the partial shrinking and the surface structure formation.

Another important point to be analysed was the preservation of the crystal structure of the LLZ and thus the electrochemical behaviour of the sintered layer. In Figure 5, the X-ray diffraction pattern for the untreated powder material and four laser sintered LLZ layers are shown (corresponding to c – f).

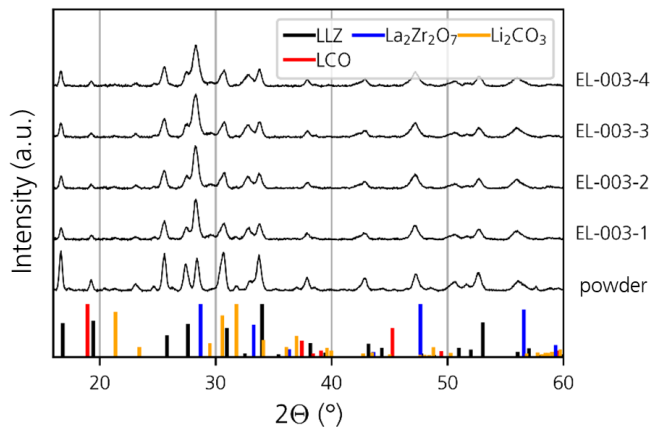


Fig. 5. XRD-pattern of the sintered LLZ layers. Different crystal structures are marked, expected is LLZ.

It can be noticed that even the powder material shows not only signals of LLZ. The signal at 28° can be attributed to the structure of lanthanum zirconate ( $\text{La}_2\text{Zr}_2\text{O}_7$ ). However, this phase, to which an ion-insulating property is attributed, is not enhanced by the sintering process. For the presented laser sintering, the LLZ phase is reduced in signal intensity but still preserved.

#### 4. Conclusion

In this paper, a new and highly scalable sintering process of ceramic thin films is presented. Therefore, a sintering process of LLZ electrolyte for solid-state batteries was carried out. It can be demonstrated that the LLZ layer was surface-near completely sintered, thermal damage was avoided. Based on the XRD – measurements, the preservation of the LLZ structure is confirmed. The thickness of the sintered layer varied over the sample between 4 – 8  $\mu\text{m}$ . With the presented excimer laser system from Coherent, we were able to achieve a processing surface rate of 62  $\text{mm}^2/\text{s}$ . This can already be increased by an order of magnitude with existing systems. The characterization of the electrochemical properties of the sintered layer and the upscaling from laboratory to industrial scale, in which several metres are processed per minute, has to be proven yet. Also, there is still potential for optimisation in terms of preserving the crystalline phase of the sintered LLZ material. The authors would like to thank the consortium for the excellent cooperation within the project “OptiKeraLyt” (funding code 03ETE016D by BMWi).

#### References

- [1] J. Schnell, T. Günther, T. Knoche, C. Vieider, L. Köhler, A. Just, M. Keller, S. Passerini, G. Reinhart, in “All-solid-state lithium-ion and lithium metal batteries – paving the way to large-scale production” *Journal of Power Sources*, Volume 382, 2018, Pages 160-175.
- [2] S. Troy, A. Schreiber, T. Reppert, H. Gehrke, M. Finsterbusch, S. Uhlenbruck, P. Stenzel, in “Life Cycle Assessment and resource analysis of all-solid-state batteries” *Applied Energy*, Volume 169, 2016, Pages 757-767.
- [3] M. Shoji, H. Munakata and K. Kanamura, in “Fabrication of All-Solid-State Lithium-Ion Cells Using Three-Dimensionally Structured Solid Electrolyte  $\text{Li}_7\text{La}_3\text{Zr}_2\text{O}_{12}$  Pellets” *Front. Energy Res.*, 2016, 4:32. doi: 10.3389/fenrg.2016.00032.
- [4] R. Delm Dahl, in “Precision Engineering” *Nature Photonics* 4, 286, (2010).